



Contents lists available at ScienceDirect

## International Journal of Industrial Ergonomics

journal homepage: [www.elsevier.com/locate/ergon](http://www.elsevier.com/locate/ergon)

## Effect of body-borne equipment on injury of military pilots and aircrew during a simulated helicopter crash



Daniel Aggromito <sup>a, b</sup>, Rodney Thomson <sup>b, c</sup>, John Wang <sup>d</sup>, Allen Chhor <sup>e</sup>, Bernard Chen <sup>a</sup>, Wenyi Yan <sup>a, \*</sup>

<sup>a</sup> Department of Mechanical & Aerospace Engineering, Monash University, Clayton, VIC 3800, Australia

<sup>b</sup> Cooperative Research Centre for Advanced Composite Structures, 1/320 Lorimer Street, Port Melbourne, VIC 3207, Australia

<sup>c</sup> Advanced Composite Structures Australia Pty Ltd, 1/320 Lorimer Street, Port Melbourne, VIC 3207, Australia

<sup>d</sup> Defence Science and Technology Organisation, 506 Lorimer Street, Fishermans Bend, VIC 3207, Australia

<sup>e</sup> Pacific ESI, 277-279 Broadway, Glebe, NSW 2007, Australia

### ARTICLE INFO

#### Article history:

Received 9 February 2015

Received in revised form

23 June 2015

Accepted 9 July 2015

Available online 23 July 2015

#### Keywords:

Helicopter

Crash

Equipment

Survival

Military

### ABSTRACT

Military helicopter pilots are expected to wear a variety of items of body-borne equipment during flight so as to be prepared for any situation that may arise in combat. Helicopter seats are designed to a specified weight range for an occupant with equipment. This paper investigates how distributing the equipment on the body affects injury potential during a helicopter crash. A finite element model representing a helicopter seat with a fully deformable 50th percentile Hybrid III carrying equipment was developed. The model was subjected to a standard military certification crash test. Various equipment configurations were investigated and analysed to determine its influence on the risk of injury. It was found that placing the equipment low on the torso, i.e. near the thighs, not only reduces the likelihood of injury in the lumbar, spinal region but also provides favourable results in neck and head injury risk when compared to other configurations investigated. In contrast, placing equipment high on the torso, i.e. close to the chin, increases the lumbar load and implicitly, the risk of head injury. A statistical analysis is carried out using the Wilcoxon Signed Rank Test to deliver probability of loads experienced within a certain interval. This study recommends an equipment configuration that improves survivability for an occupant seated on a fixed load energy absorbing seat which is subjected to Military Standard 58095A Test 4.

© 2015 Elsevier B.V. All rights reserved.

## 1. Introduction

Combat environments have evolved over the years, placing troops in a number of new and different combat situations. This has directly led to the advancement in military personnel equipment to ensure that troops are prepared for any new scenarios. When those personnel are flying in helicopters, equipment is placed on the body not only with an emphasis on easy accessibility but also an

even distribution of the load during flight to minimise cumulative loading. Helmet loads during simulated day and night flights have been studied comprehensively (Forde et al., 2011; Navy upgrading its aircrew, 2013). However, understanding the load distribution on other parts of the body and how it affects injury criteria in a helicopter crash is largely unknown. The majority of equipment carried by personnel is placed inside a primary survival gear carrier (PSGC), which sits over the top of the flight suit and the body armour on the upper torso. Inside the PSGC are placed the medical supply kit, ammunition, air bottle, radio, flashlight, survival knife and emergency signal mirror and other equipment as demonstrated in Fig. 1. Equipment weight varies, normally in the range 5 kg–30 kg, depending on what is considered essential to a specific mission (13-1-6.7-2 Aircrew, 2007). Australian Defence Personnel, use a Modular Lightweight Load Carrying Vest (MOLLE), which allows them to position pouches carrying equipment at any position, they prefer.

*Keywords abbreviation:* PSGC, Primary Survival Gear Carrier; JSSG, Joint Service Specification Guide; VPS, Virtual Performance Solutions; ATD, Anthropomorphic Test Device; FTSS, First Technology Safety Solutions; COG, Centre of Gravity; NIJ, Neck Injury Criteria; NTE, Neck Tension/Extension; NTF, Neck Tension/Flexion; NCE, Neck Compression/Extension; NCF, Neck Compression/Flexion; HIC15, Head Injury Criteria.

\* Corresponding author.

E-mail address: [WenYi.Yan@monash.edu](mailto:WenYi.Yan@monash.edu) (W. Yan).

<http://dx.doi.org/10.1016/j.ergon.2015.07.001>

0169-8141/© 2015 Elsevier B.V. All rights reserved.

In a helicopter crash, where the seat undergoes vertical loading, the design of a crashworthy seat requires that it is able to absorb the energy through a stroking load limit mechanism. This mechanism allows the seat and the occupant to move at loads that are just under the humanly tolerable limit, and over the maximum distance between the seat pan and the cabin floor. The seat is designed in terms of a specified range of occupant mass and can provide limited protection only within its designed energy absorbing capability (Desjardins, 2003). If the equipment causes the mass to increase outside the design range, a phenomenon called bottoming out will occur at the end of the stroke. Bottoming out occurs because the seat reaches its full stroking distance before the total impact energy is absorbed, resulting in the potential for a more extreme impact load and increasing the likelihood of injury. How the additional mass effects bottoming out is illustrated in a crash of a Sikorsky S-92 helicopter in which four seats bottomed-out (Transportation Safety Board of Canada (2009)). In this case, the initial vertical load factors experienced most likely exceeded 8.6 g, the seats designed limit, but were within the human tolerable limit. The primary cause of death in this situation was drowning. If this impact was to occur on land, it could be assumed that the passengers would have most likely survived with a bottoming-out load this low.

Injury from helicopter crashes can occur from a number of sources including inertial forces from excessive acceleration, blunt impact and direct contact with the vehicle, and exposure to environmental conditions such as a post-crash fire (Pellettiere et al., 2011). According to a survey that reviewed 156 US Army aviation accidents from 1983 to 2005, head/neck injury was the largest frequency with 87%, followed by injury to the spine/pelvis (83%) and to the heart/aorta (46%) (Barth and Balcena, 2010). Another review of mishap data was collected in which 917 A-B Department of Defense rotorcraft mishaps were studied covering 3800 occupant exposures. It was noted that in the Army data, the majority of fatalities had injuries to the chest, head and neck while those with only major injuries had a prevalence of upper and lower extremity injuries (Mapes et al., 2008).

Injury measurement guidelines are defined by the Federal Aviation Authority (FAA) for civil aircraft (Code of Federal Regulations) and in the Joint Service Specification Guide (JSSG) for the United States Department of Defence (DoD JSSG-2010-7, 1998). These guidelines propose a tolerance level, developed through physical testing or analysis to provide limits of human tolerance, which provides a criterion for measuring injury risk. The major areas of injury defined in these guides are related to the lumbar spine, chest, neck and head. Aircraft passenger and crew seats must complete defined dynamic tests including drop tower tests and sled tests in order to be certified. Drop tower tests use a pulse generator such as a honeycomb sandwich panel to mimic the deceleration characteristics of the cabin floor relative to the

seat when it is dropped from a predetermined height to reach the intended velocity (Chiba et al., 2014; Polanco and Littell, 2011). Sled tests apply the pulse directly to the bottom of the seat in a similar way via a propulsion method (such as bungy cords) to propel the seat to the desired velocity, which is then decelerated by the impact of honeycomb sandwich panels or hydraulic compression.

Experimental crash testing of human test subjects or crash test dummies at injury causing loads provides the ultimate validation of design effectiveness for injury risk reduction. Such methods can be ethically unsuitable or simply commercially unavailable for multiple tests. A complimentary method of analysing injury criterion of an occupant in a vertical impact crash is using crash software that utilises the explicit finite element method. For analysing a wide range of scenarios, this method is more cost effective, more time optimal, and allows detailed examination of performance not always in real life testing. Various studies have analysed seated dummies and their responses in a simulated vertical crash, with models that can vary from very simple rigid body models to very complex and detailed deformable models. Richards & Sieveka (Richards and Sieveka, 2011) modelled a UH-60 Blackhawk pilot seat. In this model, a generic floor mounted seat with rear struts supporting two guide tubes and a simple bucket were utilised and a spring device resisting the motion represented the fixed load energy absorption device. A more complex seat model for an agricultural aircraft was developed where an energy-absorbing device was modelled in LS-DYNA (Mathys and Ferguson, 2012). During the stroke, the seat slides downwards along the rails and crush the energy absorbing tubes against the fixed collars. Both studies used representative dummy models that allowed them to analyse injury during a simulated vertical crash.

A number of studies have been completed on seated dummies in landmine blasts, underwater shock and injury from aviation helmet neck loading and load carriage during walking. Further studies have been completed on the functional performance of a soldier in full chemical and biological protection. (Cheng et al., 2010; Mathys and Ferguson, 2012; Pal et al., 2014; Malapane and Shaba, 2001). However, research is limited on the effects of body-borne equipment on injury in a helicopter crash. Richards & Sieveka (Richards and Sieveka, 2011) completed a preliminary analysis of the effect of personnel equipment on injury during a helicopter crash. They used an ellipsoid Hybrid III Anthropomorphic Test Device (ATD) with a rigid lumped mass located at the centre of the sternum to represent equipment. The authors found that the lumbar load increased by at least 19% for a 50th percentile aviator to a maximum of 60%. Only the influence of one rigid upper torso equipment mass on lumbar load was considered in this study, as the major focus was the effect of various energy absorption devices used by helicopter seat manufacturers. The study concluded that lumbar load will increase with added upper torso mass. It also recommended the need for more thorough analysis including the effect of various mass properties of equipment and location to determine their influence on the major injury criteria defined by the FAA and in the JSSG. Another study completed by Aggromito et al., 2014 used a 7-degree of freedom (DOF) mass spring damper analytical model to analyse a human during a simulated helicopter crash and found that increasing equipment mass has negative effects on the onset of bottoming-out, and the forces experienced at the pelvis, upper torso and head. Both studies were limited in their analysis, indicating the need for a three-dimensional analysis. To analyse the effect of equipment on the forces on a seated person in greater detail, equipment needs to be located at a variety of locations on the body.



Fig. 1. An aircrew survival vest used by helicopter pilots (Navy upgrading its aircrew, 2013).

This study seeks to determine the effect of the mass and location of body-borne equipment on the potential injury of a dummy seated on a crashworthy seat during a simulated helicopter crash. A finite element (FE) model was developed in Virtual Performance Solution (VPS) to represent both the seat and the dummy with equipment. The FE dummy model used is a Hybrid III fully deformable 50th percentile ATD developed by FTSS. The seat is a simplified BAE UH-60 seat utilising a fixed load energy absorption device, with a load profile taken from (Aggromito et al., 2014). Tests were performed according to MIL-STD 58095A Test 4 to investigate equipment placed at various locations and representative equipment shapes.

## 2. Method

### 2.1. Seat modelling and dummy

The seat modelled in the study is a simplified Blackhawk UH-60 crew seat as shown in Fig. 2. The seat cushion and seat back cushion properties are a Sunmate memory foam, with a density of 94.8 kg/m<sup>3</sup> (Saunders et al., 2012). The stress–strain curves for the foam were taken from experimental data collected by the Defence Science and Technology Organisation (DSTO) in Saunders et al., 2012. The 75 mm thick seat cushion is connected to a rigid base at the seat back and the seat base. This connection is modelled by a tied link method, which is mesh independent so that the nodes of the connecting parts do not need to coincide (VPS Solver Notes Manual 2, 2012). In the first computational cycle, the master elements search within a specified search thickness for the connecting nodes of the part to tie. When found, these parts are linked at these node locations, allowing them to still deform independently but eliminating the need for the nodes of the two parts to be compatible (VPS Solver Notes Manual 2, 2012). The foot-well is positioned below the dummy's feet similar to the OH-58 configuration. The vertical test uses a leg configuration of approximately 135° (Haley and Palmer, 1994).

The FAA 50th percentile Hybrid III dummy is similar to the standard Hybrid III dummy used for frontal crash test, but with selected modifications for aerospace applications. A major difference is the lumbar column, which is curved on the Hybrid III, but straight on the FAA Hybrid III. The straight lumbar column allows better response measurements in vertical loading conditions. At present, an FE model of the FAA Hybrid III is not available. As a compromise, the FE model of the Hybrid III dummy was used in this

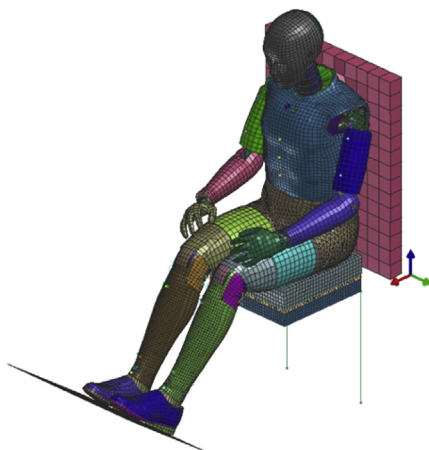


Fig. 2. Dummy on seat system used in this study.

study, which allowed a relative comparison of the effect on injury parameters of placing equipment at various locations. Only a 50<sup>th</sup> percentile version of the Hybrid III dummy is considered in this study. The primary aim is to understand how equipment mass and location effect the injury loadings on occupants. These results can be used as a guideline for the other dummy sizes such as 5th percentile and 95th percentile.

In VPS, Version 7.1.1 of the Hybrid III dummy from First Technology Safety systems (FTSS) was used. The FE model of the Hybrid III dummy is a fully deformable model consisting of 97,480 elements. The FE model has been validated on both the component level and on the sub-assembly level with the various standard dummy calibration tests (VPS Solver Notes Manual 2, 2012). The full dummy system has been validated with a thorax pendulum impact test as well as two sled tests with seat belts. The dummy has been compared with that provided by Livemore Software Technology Corporation (LTSC) and the FTSS dummy was found to provide better correlation with experimental testing. This was mainly due to the greater modelling detail in the pelvis and the inclusion of an abdomen insert which acts as a buffer to the dummy during load transfer (Polanco and Littell, 2011).

A generalised contact condition using a master and slave condition is defined between the dummy and the seat cushion and seat back, and between the feet and the foot-well. The contact condition used, automatically defines the slave and master based on the element type. The seat and dummy move in the same direction downwards and the two springs attached to the rigid plate resist the motion with a force by displacement characteristic similar to a fixed load energy absorption device. The model configuration without the seat belt is displayed in Fig. 2.

### 2.2. Acceleration pulse and stroke load profile

The dynamic crash pulse for the computer simulations is the nominal triangular test pulse from Test 4 in (Military STD 58095A, 1971), which indicates a maximum deceleration of 51 g in 0.043 s and a maximum change in velocity of 15.2 m/s, as shown in Fig. 3. The deceleration pulse is applied to the cabin floor.

The basic energy absorption profile shown in Fig. 3(b) is from Aggromito et al., 2014 with minor modifications, including an initial spike in loading after the energy absorption device first reaches the limit load. The seat is designed for the limit load to be reached quickly after only 5 mm of stroke, and to remain at that load for the duration of the stroke. If the total impact energy is not absorbed prior to the stroking limit, seat bottoming out occurs and the force increases as seen in Fig. 3(b). If the dummy has not returned to equilibrium after 374 mm of stroke, the seat system will bottom out.

### 2.3. Seat belt

A seat belt is used to hold the body into the seat and to prevent the head and upper body from flailing. Using the auto belt tool in VPS, a five-point belt was developed for use in the model. Quad elements are used to represent the belt with an element size of 10 mm. There are five connection points, four in the rigid seat back and one in the rigid seat base. A belt offset to the body of 2 mm is used. The belt uses Type 102- elastic-plastic (shell) material to simulate a nylon fabric with a Young's modulus of 13 GPa, a density of 1150 kg/m<sup>3</sup> and a yield stress of 0.221 GPa. To remove slack in the belt and to ensure that it is both tensioned and in contact with the body, the belt is first tightened by moving and stretching the belt onto the body.

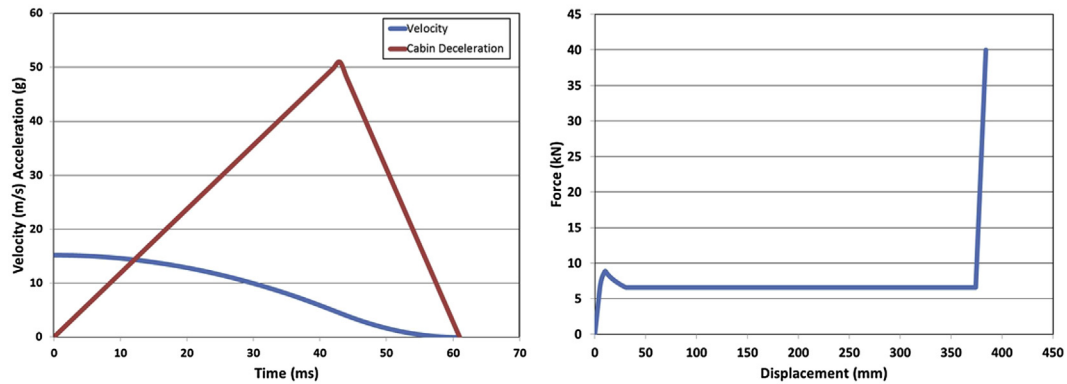


**Fig. 3.** (a) Acceleration and velocity pulse used in the analysis as defined by MIL-STD 58095A Test 4, (b) stroke versus load response of the two springs to represent the impacting motion and energy absorption.

#### 2.4. Simulation procedure

The simulation is a two-stage analysis. It begins with a pre-loading phase, allowing the dummy to settle into the seat under gravity, and the seat belt to tighten. The dummy has a total weight of 77.43 kg. The contact force between the dummy and the foam is tuned to approximately 660 N as the weight of the legs is subtracted. Stage 2 simulates the impact where the pulse and impact velocity are applied to the system as shown in Fig. 3.

The following are the characteristics of the analysis:

##### 2.4.1. Stage 1

- The dummy centre of gravity (cog) nodes have fixed boundary conditions in all directions.
- A defined displacement condition is applied on the seat to push the seat into the dummy (contact force  $\sim$  ATD mass X gravitational acceleration).
- A defined displacement condition is applied to pre-load the stroking mechanism of the seat where the dummy mass is placed.
- The aluminium bar connecting the seat belt to the seat base moves with the belt.
- The anchor points of the seat belt move in the x and z direction creating a firm contact to the body.

##### 2.4.2. Stage 2

- An initial velocity of 15.26 m/s is applied to the dummy, the seat, and all its components.
- The deceleration profile as shown in Fig. 3 is applied to the spring and foot-well.
- A constraint is placed on the connecting nodes of the aluminium bar to the fabric of the belt in all directions other than the z direction, allowing free movement in the vertical direction. This ensures the belt remains tensioned and firm across the body without any lateral slipping on the shoulders.
- The fixed condition placed on the dummy in stage 1 is removed allowing the whole dummy to freely move with respect to the contact conditions with the seat, footrest and belt restraint system. Figs. 4 and 5

#### 2.5. Model validation

To verify the modelling configuration, the model inputs were defined to match those of the models of Richards & Sieveka (Richards and Sieveka, 2011) and the results compared as shown in Table 1. The model inputs changed to match the models compared with, are the external loads, including the velocity and cabin deceleration and the stroking profile.

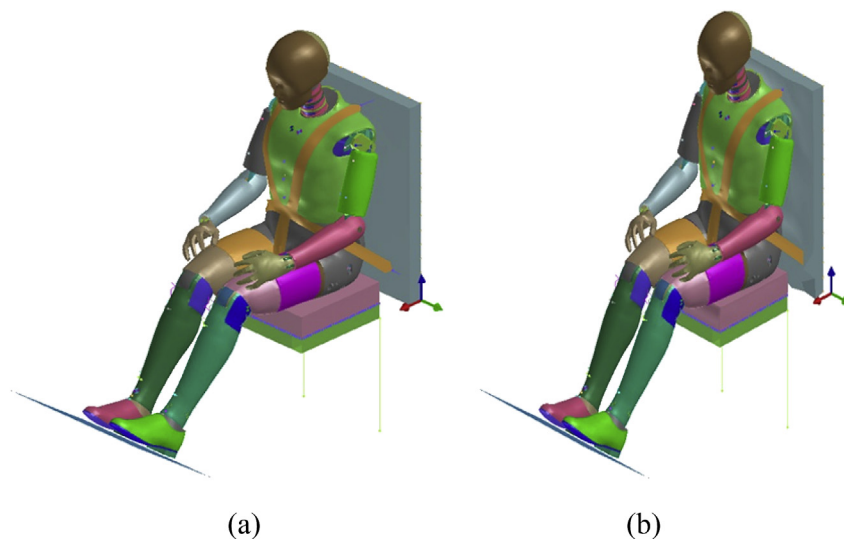


**Fig. 4.** Stage 1 of the simulation at (a) beginning (b) end positions.

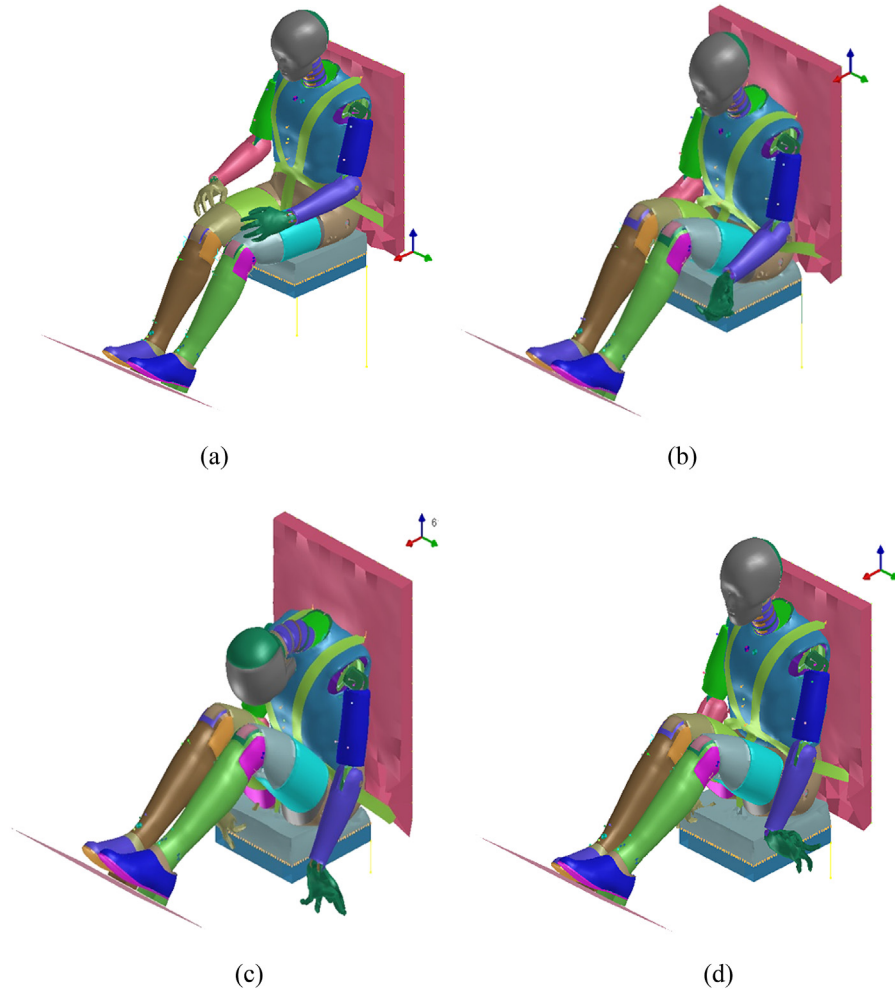


Fig. 5. Stage 2 of the simulation at (a) beginning (b) 60 ms (c) 120 ms and (d) 180 ms.

The lumbar load calculated with the fully deformable dummy was 43% lower than that reported by Richards and Sieveka, 2011 while the stroking length was 16% higher. This discrepancy could be due to the use of a fully deformable Hybrid III model in this study, whereas an ellipsoid rigid dummy was used in Richards and Sieveka, 2011. As a check, a rigid body dummy model was imported into the VPS model configuration. This produced a lumbar load increase of 20% compared to the deformable dummy model, showing that the method used to model the dummy has an effect on the lumbar loads and the stroking load. The discrepancy in

lumbar load can depend on the detail of the dummy as demonstrated by the comparison in Polanco and Littell, 2011. The model analysed here was compared with an internal report completed that investigated a dummy seated on various foam types, including the Sunmate foam used in this study, during a drop test. The results demonstrated good correlation within 10% of the experimental and numerical components completed in that study.

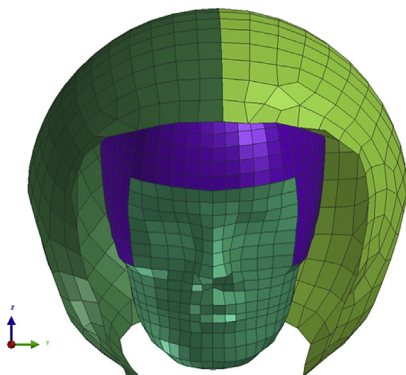


Fig. 6. Helmet connected to the Head.

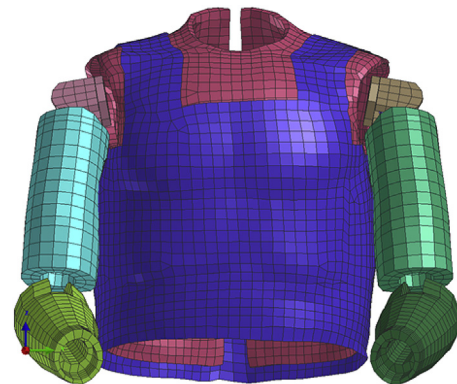


Fig. 7. The blue section represents the PSGC sitting on top of the body. (For interpretation of the references to colour in this figure legend, the reader is referred to the web version of this article.)

**Table 1**  
Validating the simulation results against Richards & Sieveka (Richards and Sieveka, 2011).

Case	Lumbar load (kN)	Stroke (mm)
Richards & Sieveka (DoD JSSG-2010-7, 1998)	10.0	299
Simulation (Rigid Ellipsoid Dummy)	7.27	262
Simulation (Fully Deformable Dummy)	5.74	347

## 2.6. Equipment modelling

### 2.6.1. Helmet

The helmet is a basic military style helmet, without night vision goggles (NVG) and counter weight (CW) balances. It has a mass of 2 kg, which fits in the range of standard helmet masses (Mathys and Ferguson, 2012). The helmet is attached to the head with 4 springs, spaced at equal points. The major concern of the study is the effect of upper torso equipment rather than the effect of the helmet mass on the head and therefore the foam of the helmet liner was not modelled. Fig. 6.

### 2.6.2. Body-borne equipment

A list of typical body-borne equipment is presented in Table 2 (Richards and Sieveka, 2011). The flight suit and body armour are added to the body as a mass distributed all over the upper torso. To reduce computing time, body-borne equipment is represented as non-deformable bodies.

### 2.6.3. Primary survival gear carrier

In the simulation, the PSGC sits 1 mm from the body. A general contact condition exists between the PSGC and the body to represent the PSGC sitting on the upper torso. The PSGC is modelled using shell elements with an element size of 10 mm. The carbon fibre filled Nylon 6 PSGC has an elastic modulus of 9 GPa and a density of 1190 kg/m<sup>3</sup>. The equipment is attached using a tied link with a non-damaging interface, providing an attachment that does not fail under load. Fig. 7.

## 2.7. Injury criteria used in the analysis

The injury criteria assessed in the analysis are summarised in Table 3. Inbuilt in the Hybrid III dummy supplied by FTSS is a lumbar spine load cell located 15 mm below the lumbar spine. This load cell allows a fully 3-Dimensional calculation of the lumbar force. Chest injury can occur through direct impact or from inertial forces. Inertial loading of the chest is a result of rapid deceleration of the occupant and interaction with the restraint system.

To analyse neck injury, the Neck Injury Criterion (NIJ) is used. Injuries to the neck can occur from multiple loading scenarios with typical injuries being vertebral fractures, dislocations and a basilar

skull fracture, which can occur from excessive loading to the neck (Pellettiere et al., 2011). The neck injury criterion gauges injury for the loading situations including tension/extension (NTE), tension/flexion (NTF), compression/extension (NCE) and compression/flexion (NCF). The NIJ is calculated using the following equation:

$$N_{ij} = \left| \left( \frac{F_z}{F_{int}} \right) \right| + \left| \left( \frac{M_y}{M_{int}} \right) \right| \quad (1)$$

Where  $F_z$  is the axial tension/compression load,  $F_{int}$  is the critical intercept load,  $M_y$  is the flexion/extension bending moment and  $M_{int}$  is the critical intercept moment.

Head injury is calculated based on a particular linear acceleration of the head using the Head Injury Criterion (HIC15). This measures the change in acceleration during a 15-ms window. The criterion requires that HIC15 shall not exceed 700. The HIC15 is calculated using the following formula:

$$HIC = \left[ \frac{1}{(t_2 - t_1)} \int_{t_1}^{t_2} a dt \right]^{2.5} (t_2 - t_1) \quad (2)$$

where  $a$  is the resultant acceleration exposed as a multiple of  $g$ , and  $t_1$  and  $t_2$  are any two points in time during the acceleration of the head. These points are not separated by more than a 15-ms interval and are chosen such that the maximum possible value of the HIC15 is calculated.

**Table 3**  
Injury threshold values.

Injury	Threshold
Lumbar Load (kN)	9.2
Chest Injury (kN)	8.90
<b>Neck Injury</b>	
Tension (kN)	4.5
Compression (kN)	4.5
Flexion (Nm)	310
Extension (Nm)	125
Head Injury Criterion (HIC15)	700

**Table 2**  
Data of equipment items used in the study (Richards and Sieveka, 2011).

Item	Approximate area (m <sup>2</sup> )	Mass (kg)
Helmet	0.1839	2
Body Armour and Flight Suit	N/A	6.53
First Aid Kit	0.02	1.06
Flotation Collar	0.057	1.53
Misc Pouch with Magazine and Signal Flares	0.00894	0.19
Accessories Pouch	0.01557	1
Accessories Kit	0.009	1.04
Radio	0.009	0.25
Air Bottle	0.015	0.42
Gun	0.0175	2.04
Knife Pouch with Knife	0.015	0.2
Total		16.26

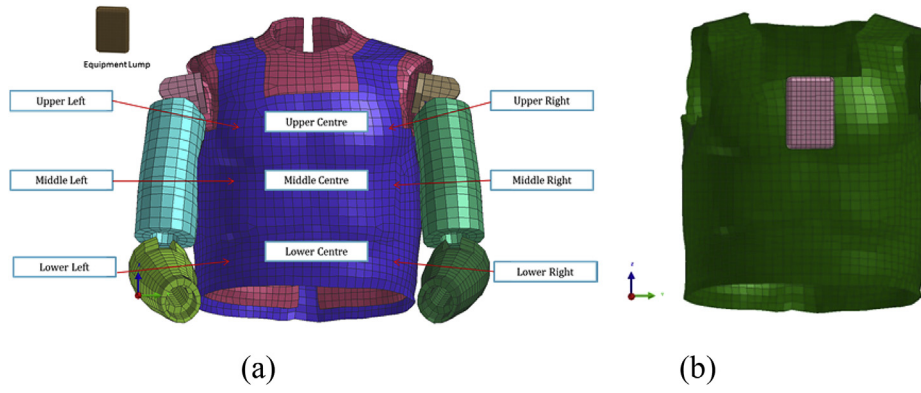


Fig. 8. (a) Equipment mass locations (b) An illustration of how the single equipment mass is attached to the PSGC.

2.8. Investigation of equipment configuration using lumped masses

To determine the effect of equipment on injury during a simulated helicopter crash, initial simulation cases to determine basic trends were carried out using only one piece of equipment at

different locations, then gradually incorporating additional equipment combinations. Initially, a single 10 kg equipment mass was placed at various locations on the PSGC as a preliminary analysis. Following this, two 5 kg equipment masses were placed at various locations on the upper torso. Finally, three equipment masses were

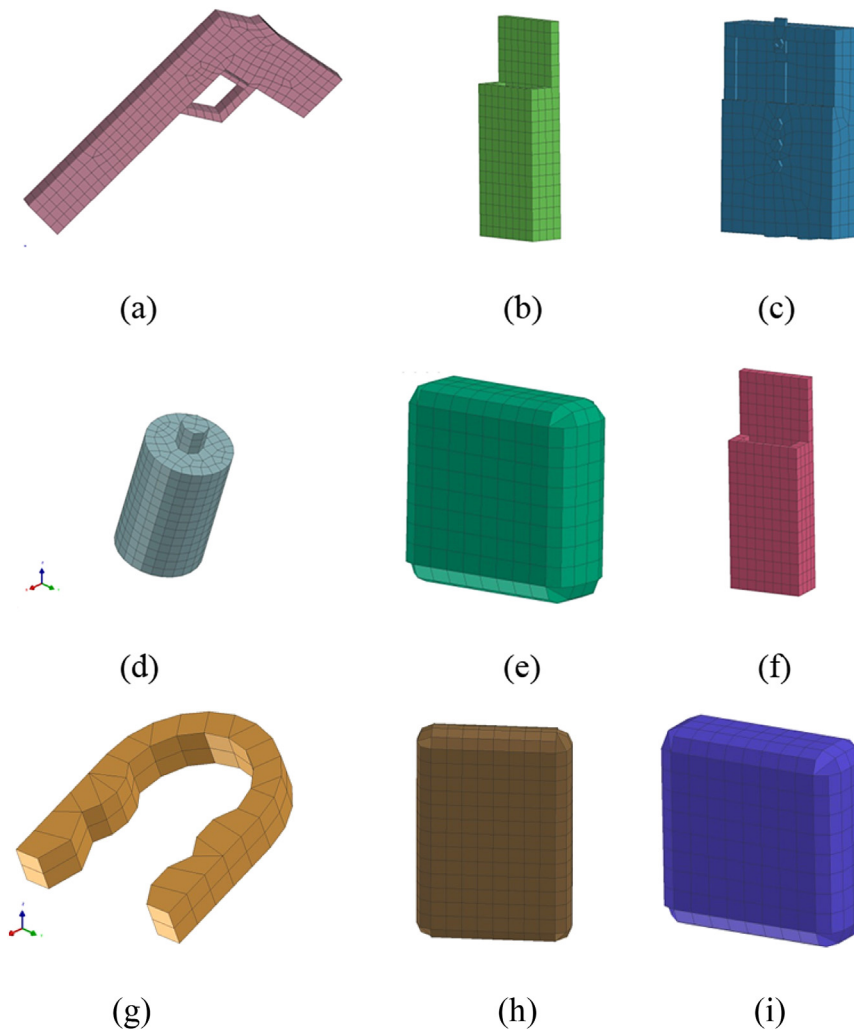


Fig. 9. Models of (a) Gun (b) Knife Pouch (c) Radio (d) Air Bottle (e) First Aid Kit (f) Magazine Pouch (g) Flotation Collar (h) Accessories Pouch (i) Accessories Kit used in the simulations.

placed on the upper torso, each weighing 3 kg. Fig. 8 illustrates the terminology used for each simulation case investigated in the preliminary analysis.

It should also be noted that the body armour, the flotation collar and the helmet were considered essential equipment and therefore remained on the body in these analyses.

2.9. Representative equipment on the body

To validate the findings from the preliminary analysis, a more detailed analysis was completed in which representative shapes and masses are used to represent the body-borne equipment used by military pilots. The shape, size and mass of the equipment listed in Table 2 were modelled as shown in Fig. 9.

While a vast number of equipment configurations are possible, the configurations shown in Fig. 10 were investigated.

3. Results

3.1. Results without equipment

An initial simulation without equipment was carried out to establish a reference case allowing load changes to be assessed for

subsequent simulations with equipment. Table 4 shows the results for the dummy in the crash case without equipment.

As can be seen from Table 4, the ATD without equipment does not exceed any of the injury threshold values defined in the FAA and JSSG standard.

3.2. Major findings of the lumped mass analysis

The initial lumped analysis is summarized in Tables 5–8. This analysis demonstrates that placing the equipment lump in the centre, and at the top, of the torso will generate the highest lumbar load (upper centre according to Fig. 8(a)), the greatest loading in the torso strap, and the highest flexion of the neck. HIC increases substantially when the equipment lump is placed in the centre of the body and at the upper right/upper left. When the equipment is placed in the lower part of the torso, the extension criterion of the NIJ is the highest.

In contrast, placing the equipment on the lower right/lower left generates the lowest lumbar load, NIJ for neck and HIC. The seat belt load decreases when the equipment is placed on the lower right/lower left of the body. However, when placed in the centre of the body, the seat belt load increases.

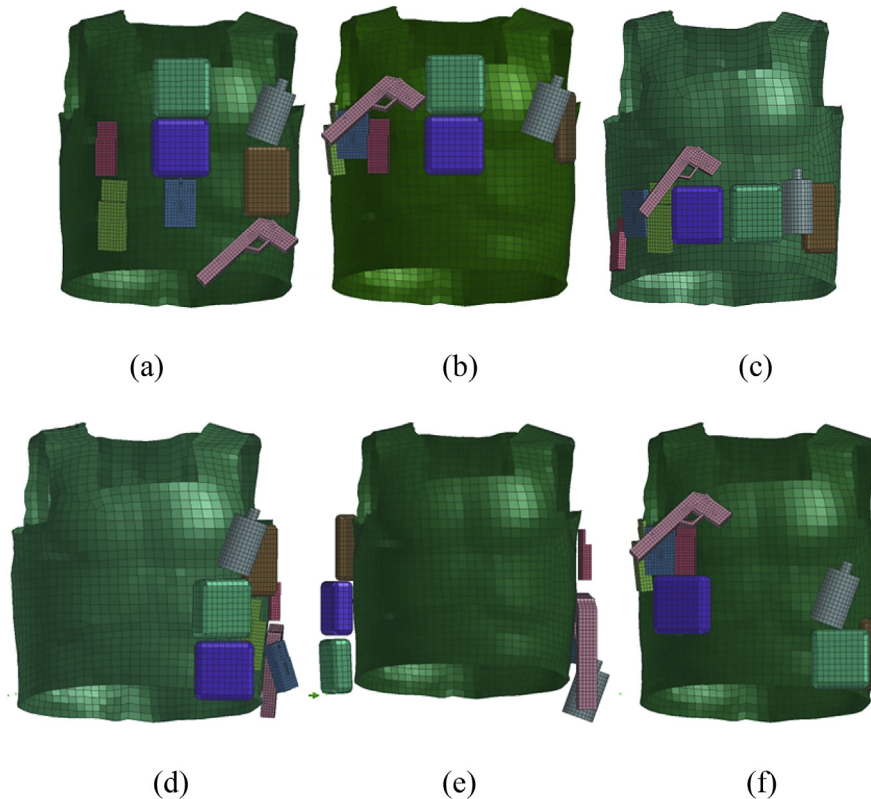


Fig. 10. Investigated equipment configurations: (a) middle of the body (b) top distributed (c) low distributed (d) located on one side (e) located on either side of the body (f) located diagonally across the body.

Table 4  
Simulation results without equipment.

Simulation case	Lumbar load (kN)	Load on belt strap (kN)	Neck injury	HIC15
No Equipment	7.02	3.19	NTE = 0.46 NTF = 0.58 NCE = 0.78 NCF = 0.65	200

**Table 5**  
Single lumped mass with a mass of 10 kg at the different locations of Fig. 8.

Simulation case	Lumbar load (kN)	Load on belt strap (kN)	Neck injury	HIC15
Lower centre	11.9	5.93	NTE = 1.12; NTF = 1.51 NCE = 1.89; NCF = 0.95	698
Middle centre	11.8	7.07	NTE = 0.93; NTF = 1.6; NCE = 1.83; NCF = 0.95	691
Upper centre	14.4	8.18	NTE = 0.82; NTF = 2.03 NCE = 1.40; NCF = 1.54	681
Lower right	8.3	5.69	NTE = 1.1; NTF = 1.2 NCE = 1.83; NCF = 0.91	621
Middle right	10.7	5.57	NTE = 0.83; NTF = 1.44 NCE = 1.85; NCF = 0.94	691
Upper right	11.8	6.48	NTE = 0.94; NTF = 1.44 NCE = 1.54; NCF = 0.95	697

**Table 6**  
Two lumped masses of 5 kg each; one located at 'Upper right' and the other at different locations of Fig. 8.

Simulation case	Lumbar load (kN)	Load on belt strap (kN)	Neck injury	HIC15
Lower centre	9.97	8.8	NTE = 0.69; NTF = 1.33 NCE = 1.89; NCF = 0.94	695
Middle centre	9.5	7.83	NTE = 0.92; NTF = 1.81 NCE = 1.91; NCF = 0.96	703
Upper centre	14.4	8.21	NTE = 0.99; NTF = 1.50 NCE = 1.70; NCF = 0.95	706
Upper left	12.42	6.08	NTE = 0.93; NTF = 1.28 NCE = 1.75; NCF = 0.95	702

**Table 7**  
Two lumped masses of 5 kg each; one located at 'Lower right' and the other at the different locations of Fig. 8.

Simulation case	Lumbar load (kN)	Load on belt strap (kN)	Neck injury	HIC15
Upper left	9.38	7.23	NTE = 0.98; NTF = 1.19 NCE = 2.13; NCF = 0.94	686
Lower left	11.76	4.12	NTE = 0.73; NTF = 0.92 NCE = 1.85; NCF = 0.95	711
Lower centre	10.66	7.22	NTE = 0.62; NTF = 1.73 NCE = 1.40; NCF = 0.81	490
Middle centre	11.48	6.25	NTE = 0.71; NTF = 1.66 NCE = 1.45; NCF = 0.94	670
Upper centre	11.4	5.61	NTE = 0.60; NTF = 1.18 NCE = 1.70; NCF = 0.90	621
Upper right	10.36	4.58	NTE = 1.07; NTF = 1.18 NCE = 1.90; NCF = 0.91	626

**Table 8**  
Three lumped masses of 3 kg each; located at the different locations of Fig. 8.

Simulation case	Lumbar load (kN)	Load on belt strap (kN)	Neck injury	HIC15
Upper right–Upper centre–Upper left	11.88	12.78	NTE = 0.71; NTF = 1.82 NCE = 1.65; NCF = 0.96	707
Upper right–Lower centre–Upper left	11.6	7.41	NTE = 1.02; NTF = 1.61 NCE = 1.73; NCF = 0.96	696
Upper right–Middle centre–Upper left	11.29	7.78	NTE = 0.69; NTF = 1.71 NCE = 1.81; NCF = 0.93	687
Lower right–Lower centre–Lower Left	10.4	6.9	NTE = 0.94; NTF = 1.26 NCE = 2.08; NCF = 0.96	689
Lower right–Middle centre–Lower left	10.53	7.99	NTE = 0.69; NTF = 1.93 NCE = 1.96; NCF = 0.95	687
Lower right–Upper centre–Lower left	12.64	6.87	NTE = 0.86; NTF = 1.56 NCE = 1.84; NCF = 0.95	700
Upper right–Upper centre–Lower left	11.78	10.61	NTE = 0.83; NTF = 2.01 NCE = 1.53; NCF = 0.95	691
Upper right–Upper centre–Lower centre	11.13	8.38	NTE = 0.98; NTF = 1.25 NCE = 1.63; NCF = 0.95	712
Upper right–Upper centre–Middle centre	11.52	7.14	NTE = 0.91; NTF = 1.62 NCE = 1.53; NCF = 0.96	706
Upper right–Middle centre–Lower centre	10.79	6.6	NTE = 0.80; NTF = 1.58 NCE = 1.85; NCF = 0.95	694

### 3.3. Comparing the bulk/shape of equipment

The bulk/shape of the equipment has an influence on the lumbar load experienced in the x and z directions as shown in Table 9. A single lumped mass of 10 kg was placed at the lower centre and the area associated with the mass was altered. It was found that an increase in area resulted in higher lumbar loads in the x and z directions.

### 3.4. Understanding the effect of bottoming out on seat parameters

The effect of equipment location on the predicted seat load was also analysed and the results presented in Table 10. The lumbar load

increases once bottoming-out occurs. The earlier bottoming-out occurs, the higher the lumbar load recorded.

### 3.5. Comparing the friction coefficient of the PSGC and its effects

The friction coefficient between the PSGC and the body has an effect on the injury criteria value measured, as demonstrated in Table 11. A higher friction coefficient increases the lumbar load, but reduces the HIC15 and the neck extension injury values. The HIC15 decreases as the PSGC is less prone to sliding up the upper torso, causing the mass of the equipment to be carried predominately by the upper torso.

**Table 9**  
Comparing the bulk of the equipment shape.

Lump type	Lumbar load X (kN)	Lumbar load Z (kN)	Curvature of the lumbar spine (mm)
Modular Pouch (Area = 15571.5 mm <sup>2</sup> )	5.71	10.4	30.8
Medical Supply Kit (19993.7 mm <sup>2</sup> )	6.86	10.33	30.84
Medical Supply Kit (Area decreased by 8747.2 mm <sup>2</sup> )	5.5	9.07	30.27
Medical Supply Kit (Area increased by 8797.2 mm <sup>2</sup> )	6.9	11.9	31.05

**Table 10**  
Seat parameters.

Equipment location	Time at which bottoming-out occurs (ms)	Lumbar load magnitude (kN)	Seat load at max lumbar load (kN)	Time (ms) at maximum lumbar load
Lower centre	87.8	11.9	30.19	91
Middle centre	86.65	11.77	30.47	91.13
Upper centre	86.9	14.42	29.67	90.92
Lower right <sup>a</sup>	87.95	8.3	7.71	37.7
Middle right	87.12	10.7	31.6	91.45
Upper right	86.35	11.8	31.27	90.97

<sup>a</sup> Never experiences the bottoming-out condition.

**Table 11**  
Comparing the friction coefficient of the contact between the PSGC and the body.

Simulation case	Lumbar load (kN)	Load on belt strap (kN)	Neck injury	HIC15
No friction coefficient	11.9	5.93	NTE = 1.12; NTF = 1.51 NCE = 1.89; NCF = 0.95	698
0.2 friction coefficient	13.1	7.96	NTE = 0.98; NTF = 1.86 NCE = 1.43; NCF = 1.43	683
1 friction coefficient	20.65	7.30	NTE = 0.59; NTF = 2.06 NCE = 0.91; NCF = 1.21	494

### 3.6. Results from the study using representative equipment shapes

The following are the results from the equipment configurations in Fig. 10. The “equipment located on one side” generates the lowest lumbar load as the majority of the equipment mass is located far from the centre of the upper torso. In contrast, placing equipment at the centre of the body generates the highest lumbar load, as the majority of the equipment mass is located through the loading path of the lumbar spine. Equipment located on either side of the body creates the lowest HIC15 as a result of the equipment being located far from the chin. The middle of the body configuration generates the highest HIC15 and NTE is at a maximum when equipment is located lower on the torso. These findings validate the initial lumped mass analysis. Table 12.

### 3.7. Injury criteria

The analysis shows that greater lumbar loads are generated when the equipment is placed in the upper centre of the sternum compared with other locations. When utilising representative shapes for the equipment, similar results were found. The reason for this is that the loads induced by the equipment pass straight through the lumbar load cell. Therefore, it is beneficial to place equipment mass lower on the body and either side of the sternum. This results in lower lumbar loads and therefore an improved likelihood of preventing spinal injury. Furthermore, contact between the legs and the equipment was found beneficial in reducing the lumbar load due to the development of a load path that circumvents the lumbar.

The Wilcoxon Signed Rank Test is used to determine the confidence interval of where the injury risk may fall depending on location of the equipment mass. This test is a non-parametric test that does not make any assumptions on the distribution and assumes independence. A Wilcoxon signed rank test based on the

torso location of the mass was completed for the results of lumbar load, belt strap load, HIC and NIJ injury criteria. This included all the results from Tables 5–8. Two cases were compared. For the lumbar load investigation, the first case considered all simulations that included at least one mass at the upper centre, while the second case considered all cases where a pouch was located at the lower section of the lower torso. For the other injury results, the first case included all simulations that included at least one mass at the upper section of the upper torso (upper right, upper centre and upper left), while the second case considered all cases where a pouch was located at the lower section of the lower torso.

The results of the analysis indicate that if one mass is located in the upper centre of the torso, there is an achieved confidence of 95.6 that the lumbar load measured will fall within 11.31 kN and 14.40 kN. If the mass is located lower on the torso, there is an achieved confidence of 95.5 that the lumbar load measured will be within 9.89 kN and 11.48 kN. The analysis demonstrates that wearing equipment high on the torso will generate a higher loading on the lumbar spine during a vertical crash test, however, when the dummy is wearing the equipment at a lower position on the torso, the loads experienced are reduced. Table 13.

The load in the seat belt is mainly affected by the height of the equipment on the body. The higher the equipment is positioned, the higher the load on the seat belt. Furthermore, placing equipment closer to the shoulder leads to an even higher load on the seat belt, due to the body's tendency to twist.

As shown in Table 14, if the mass is located in the top part of the body, the load in the belt strap will be greater than if it was located lower, with a considerable increase in the estimated medians and the upper limit of the confidence interval.

Neck injury is affected primarily by helmet mass, where an increase in NTE, NTF, NCE and NCF was noted when the helmet mass was increased by 0.5 kg. This condition produces greater

**Table 12**  
Representative equipment Configuration results.

Simulation case	Lumbar load (kN)	Load on belt strap (kN)	Neck injury	HIC15
Middle of the Body	13.52	6.73	NTE = 0.58; NTF = 1.15 NCE = 1.43; NCF = 0.94	692
Top Distributed	9.33	6.93	NTE = 0.91; NTF = 1.44 NCE = 1.61; NCF = 0.78	503
Low Distributed	10.57	4.6	NTE = 1.07; NTF = 1.11 NCE = 1.60; NCF = 0.91	681
One side of the body	8.74	6.39	NTE = 0.53; NTF = 1.42 NCE = 1.61; NCF = 0.93	674
Either side of the body	12.99	6.48	NTE = 0.77; NTF = 1.10 NCE = 1.12; NCF = 0.72	400
Diagonally across the body	11.2	669	NTE = 0.60; NTF = 1.36 NCE = 1.08; NCF = 0.89	7.35

**Table 13**  
Wilcoxon Signed Rank Non-Parametric Analysis of lumped mass analysis for Lumbar Load Results.

Simulation case	Number of cases	Estimated median (kN)	Achieved confidence (%)	Confidence interval lower (kN)	Upper (kN)
Mass located on Upper Centre	9	12.76	95.6	11.31	14.40
Mass located on lower section of the upper torso	11	10.76	95.5	9.89	11.48

lateral movement of the head, causing the head, and therefore the neck, to extend. If the equipment is placed mainly on the centre of the body, the flexion criteria is increased as the head bends further into the body causing increased neck flexure. As shown in Table 15, the estimated median is larger for the NTE, NTF and NCE when the mass is located on the lower section of the upper torso, however the estimated median for NCF does not show a major difference.

HIC15 is affected primarily by helmet mass; however, the location of equipment on the upper torso also has an effect. This effect is demonstrated when the “low symmetry” configuration is modified so that the air bottle is moved close to the chin, which increases the HIC15 by 40. Placing equipment high and at the centre of the upper torso increases the HIC15.

Table 16 shows small differences between HIC15 for the lumped mass analysis, with only a small increase in the median value when the mass is located on the upper section of the torso. This indicates that HIC15 being mainly influenced by helmet mass.

## 4. Discussion

### 4.1. Effect of bulk/shape of equipment

The bulkier shape causes the posture of the dummy to move forward, thus creating a greater load on the lumbar spine. Compression of the lumbar spine also increases as the equipment becomes bulkier.

**Table 14**  
Wilcoxon Signed Rank Non- Parametric Analysis of lumped mass analysis for belt strap loads.

Simulation case	Number of cases	Estimated median (kN)	Achieved confidence (%)	Confidence interval lower (kN)	Upper (kN)
Mass located on the upper section of the upper torso	19	7.32	94.9	6.65	8.18
Mass located on lower section of the upper torso	7	6.39	94.1	5.29	7.22

**Table 15**  
Wilcoxon Signed Rank Non- Parametric Analysis of lumped mass analysis for Neck Injury.

Simulation case	Number of cases	Estimated median	Achieved confidence (%)	Confidence interval lower	Upper
<b>Neck Injury Tension/Extension</b>					
Mass located in the upper section of the upper torso	19	0.857	94.9	0.800	0.925
Mass located in lower section of the upper torso	7	0.883	94.8	0.675	1.100
<b>Neck Injury Tension/Flexion</b>					
Mass located in the upper section of the upper torso	19	1.530	94.9	1.40	1.660
Mass located in lower section of the upper torso	7	1.567	94.1	1.215	1.730
<b>Neck Injury Compression/Extension</b>					
Mass located in the upper section of the upper torso	19	1.725	94.9	1.635	1.825
Mass located in lower section of the upper torso	7	1.752	94.1	1.520	1.960
<b>Neck Injury Compression/Flexion</b>					
Mass located in the upper section of the upper torso	19	0.95	94.9	0.9450	0.960
Mass located in lower section of the upper torso	7	0.945	94.1	0.88	0.95

**Table 16**  
Wilcoxon signed rank Non- Parametric analysis of lumped mass analysis for HIC15.

Simulation case	Number of cases	Estimated median	Achieved confidence (%)	Confidence interval lower	Upper
Mass located on the upper section of the upper torso	19	698.3	94.9	692.0	703
Mass located on lower section of the upper torso	7	687	94.8	589	700

### 4.2. Seat load

The effect of bottoming-out was investigated by the authors in Aggromito et al. (Pal et al., 2014) where it was found that the seat load increases substantially once bottoming-out occurs. This has a negative influence on the injury parameters. This behaviour was confirmed in the current study, where the peak injury criteria values were recorded during the bottoming-out period. “The Pearson’s correlation study was used to determine if there was a correlation between seat load and lumbar load. This method measures the dependence between two variables and assigns a value between  $-1$  and  $+1$ , where  $+1$  is total positive correlation,  $0$  is no correlation and  $-1$  is total negative correlation (Sprinthall, 2003). The lumped mass analysis carried out here showed no direct correlation between seat load and lumbar load magnitude, registering a Pearson correlation value of 0.422. As the seat load increases, though, the Pearson correlation value indicates that the lumbar load will increase. However, this result is directly affected by the loads experienced by the dummy if bottoming-out occurs. A further correlation study was therefore conducted on the seat load and the time at which maximum lumbar load occurs, and a Pearson correlation value of 0.979 was calculated, indicating, that time at maximum lumbar load correlates directly to the seat load. This agrees with Aggromito et al., 2014 in that the earlier that the bottoming-out condition occurs, the greater the chance that the lumbar loads will increase. Unlike that model, however, there are

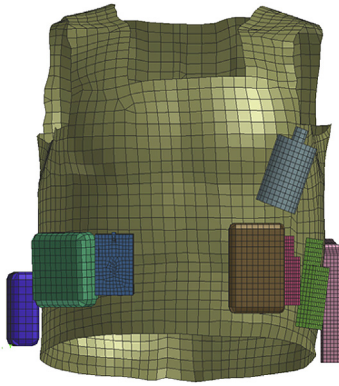


Fig. 11. Recommended Configuration.

also other important factors that contribute to the increase in lumbar load such as the equipment location. Table 10 shows the minute differences in seat load at max lumbar load and the time at which the bottoming-out condition occurs.

#### 4.3. Limitations

With any numerical method, there are obvious limitations in its ability to completely simulate the real physical situation. In reality the equipment is deformable. However, due to difficulty in obtaining equipment material properties, the equipment mass and its inertia was considered more critical in this analysis rather than the shape or the deformed shape. Furthermore, to improve computing time, springs were used to connect the helmet to the head, instead of creating a helmet liner. This is an over simplification of the helmet liner but not considered critical as the helmet to head interaction is not crucial to the study. Finally, the lumbar spine of the Hybrid III dummy is curved while the preferred FAA Hybrid III dummy designed for vertical drop tests uses a straight lumbar spine.

#### 5. Recommended configuration

The recommended configuration is developed based on the major findings from the analysis and is shown in Fig. 11. Aircrew and pilots of the Australian Defence Force use the MOLLE configuration. The results of this investigation can be used as a guide on the position that various equipment pouches should be placed to minimise injury criteria values. These findings serves as a guide on where various equipment pouches should be placed to minimise the various injury criterion. The pouch analysis demonstrated that placing equipment lower on the body, and closer to the sides, reduce risk measures such as the lumbar load and HIC15. The majority of the equipment is located lower on the body, on either side of the sternum. The heavier equipment items such as the gun and the survival and medical supply kits are placed further from the lumbar spine to reduce the loading on the lumbar region allowing the thighs to carry the loading of these equipment items. Equipment high on the centre of the torso increases the HIC15, so placing equipment in this position was avoided. This configuration takes into account ease of accessibility for the occupant, allowing them to

easily access the equipment during a crash situation. As with the other configurations, the body armour, flotation collar and helmet were unaltered.

The following guidelines for equipment placement are recommended.

- The gun should be placed on the side of the upper torso and low for easy access
- The radio should be located low on the body, at the front, due to its low mass and easy access to radio back to base.
- The magazine pouch should be located close to the weapon along with the knife pouch
- The brown accessories pouch should also be close to the front for easy access with the first aid kit on the opposite side.
- Another accessories kit should be placed on the side of the body
- The air bottle is close to the head for ease of use and quick access, its relatively low mass and does not have a major effect on the loading of the spinal column.
- The first aid kit and survival kit can be accessories pouch can be altered between the three, depending on the occupant.
- Further magazine pouches can be included and added, but placed next to the current magazine pouch and away from the lumbar spine
- The neck extension/flexion criteria can be altered by changing the counter weights and helmet used.

The results in Table 17 show the injury results for the recommended configuration.

#### 6. Conclusions

An investigation into the effect of body-borne equipment on the likelihood of injury during a helicopter crash has been investigated using numerical modelling. A finite element model of a Hybrid III dummy with equipment seated on a BAE UH-60 helicopter seat was subjected to a pulse equivalent to that of the MIL-STD 58095A crash Test 4. The model was correlated to existing literature as well as experimental tests. The following conclusions can be drawn from the investigation:

- When the equipment is placed in the upper centre of the sternum, the lumbar load will increase. Seat load is found to not have a major influence on lumbar loads. However, when the equipment is placed at the centre of the sternum, the seat load is the highest and the lumbar load is also at a maximum.
- The load in the seat belt is greater when the equipment is placed higher on the body.
- Neck injury is affected primarily by the mass of the helmet. However, when the equipment is placed lower on the torso, in particular at the lower right/lower left, the NTE is at its greatest. Flexion increases when the equipment is placed/located on the centre of the sternum.
- HIC15 is affected primarily by helmet mass; however, the HIC15 is also increased if equipment is placed in the centre of the upper torso.
- The bulk/shape of the equipment has a major effect on the lumbar load experienced in the x and z direction

Table 17  
Recommended Configuration results.

Equipment location	Lumbar load (kN)	Load on belt strap (kN)	Neck injury	HIC15
Recommended Configuration	9.2	6	NTE = 0.7; NTF = 1.2 NCE = 1.68; NCF = 0.94	678

- Friction coefficient between the contact of the PSGC and the body has an effect on the loading experienced by the lumbar spine, thus indicating the effect of the PSGC material
- A Wilcoxon Signed Rank test was completed to determine confidence intervals based on the location of the mass on the torso. The results of the test indicate that the estimated median and the confidence interval vary heavily based on which position the equipment mass is located.

The study shows that the mass distribution can potentially influence injury criteria during a simulated helicopter crash. From the major findings of the analysis, a recommended configuration and guidelines were developed on where to place the equipment in order to register loads that are below the injury criteria threshold.

### Acknowledgements

This work was undertaken as part of the Systems for Crashworthiness research project of the CRC-ACS, established and supported under the Australian Government's Cooperative Research Centres Program.

### References

- NAVAIR 13-1-6.7-2 Aircrew Personal Protective Equipment (Clothing), 2007.
- Aggromito, D., Chen, B., Thomson, R., Wang, J., Yan, W., 2014. Effects of body-borne equipment on occupant forces during a simulated helicopter crash. *Int. J. Industrial Ergonomics* 44 (4), 561–569.
- Barth, T., Balcena, P., 2010. Comparison of heart and aortic injuries to head neck, and spine injuries in US army aircraft accidents from 1983 to 2005. In: American Helicopter Society Annual Forum 66.
- Cheng, M., Phillippe Dionne, J., Makris, A., 2010. On drop-tower test methodology for blast mitigation seat evaluation. *Int. J. Impact Eng.* 37, 1180–1187.
- Chiba, M., Okino, T., Nambu, Y., Yutani, H., Katayama, K., 2014. Piled-up configuration design of decelerators in drop test for aircraft seats. *Int. J. Impact Eng.* 64, 1–19.
- Code of Federal Regulations, Title 14 Part 27.562, Airworthiness Standards: normal Category Rotorcraft Emergency Landing Dynamic Conditions.
- Desjardins, S., 2003. The evolution of energy absorption systems for crashworthy helicopter seats. In: American Helicopter Society 59th Annual Forum.
- DoD JSSG-2010-7, 1998. Crew Systems Crash Protection Handbook. Aeronautical Systems Center, ctoberWright-Patterson AFB, OH, O, p. 34.
- Forde, K.A., Albert, W.J., Harrison, M.F., Neary, J.P., Croll, J., Callaghan, J.P., 2011. Neck loads and posture exposure of helicopter pilots during simulated day and night flights. *Int. J. Industrial Ergonomics* 41, 128–135.
- Haley Jr., J.L., Palmer, R.W., 1994. Evaluation of a Retrofit OH-58 Pilot's Seat to Prevent Back Injury. USAARL Report No. 95–9.
- Malapane, N.C., Shaba, M.N., 2001. Comparison of functional performance of a soldier in full chemical and biological protection versus battle dress. *Int. J. Industrial Ergonomics* 27, 393–398.
- Mapes, P., Kent, R., Wood, R., 2008. DoD helicopter mishaps FY85–05: findings and recommendations. In: Defense Safety Oversight Council OSD 09-5-1351.
- Mathys, R., Ferguson, S.J., 2012. Simulation of the effects of different pilot helmets on neck loading during air combat. *J. Biomechanics* 45, 2362–2367.
- Military Specification, MIL-s-58095A, Seat System Crash Resistant, Non-Ejection, Aircrew, General Specification for, August 1971.
- Navy Upgrading its Aircrew Survival Vest <http://kitup.military.com/2013/12/navy-upgrading-aircrew-survival.html>.
- VPS Solver Notes Manual, 2012.
- Pal, M.S., Majumdar, D., Pramanik, A., Chowdhury, B., Majumdar, D., 2014. Optimum load for carriage by Indian soldiers on different uphill gradients at specified walking speed. *Int. J. Industrial Ergonomics* 44, 260–265.
- Pelletiere, J., Crocco, J., Jackson, K., 2011. Rotorcraft full spectrum crashworthiness and occupant injury requirements. In: American Helicopter Society 67th Annual Forum.
- Polanco, M., Littell, D., 2011. Vertical drop testing and simulation of anthropomorphic test devices. In: American Helicopter Society Annual Forum 67th.
- Richards, M., Sieveka, E., 2011. The effects of body-borne equipment weight on ATD lumbar loads measured during crashworthy seat vertical dynamic tests. In: American Helicopter Society 67th Annual Forum.
- Saunders, L., Wang, J., Slater, D., Van de Berg, J., 2012. Visco-elastic polyurethane foam as an injury mitigation device in military aircraft seating. *J. Battlef. Technol.* 15 (2), 1–8.
- Sprinthall, R.C., 2003. *Statistical Analysis*. Publishing Allyn & Bacon, Boston, MA.
- Transportation Safety Board of Canada, 2009. Main Gearbox Malfunction/collision with Water. Report number A09A0016. Cougar helicopters Inc.